

# Modelling the hysteresis in the velocity pattern of slow-moving earth flows: the role of excess pore pressure

T. W. J. van Asch\*

Utrecht Centre for the Environment and Landscape Dynamics, Heidelberglaan 2, 3584 CS Utrecht University, The Netherlands

\*Correspondence to: Th. W. J. van Asch, Utrecht Centre for the Environment and Landscape Dynamics, Heidelberglaan 2, 3584 CS Utrecht University, The Netherlands. E-mail: t.vanasch@geog.uu.nl

## Abstract

This paper describes the velocity pattern of a slow-moving earth flow containing a viscous shear band and a more or less rigid landslide body on top. In the case of small groundwater fluctuations, Bingham's law may describe the velocity of these slow-moving landslides, with velocity as a linear function of excess shear stress. Many authors have stated that in most cases a non-linear version of Bingham's law best describes the moving pattern of these earth flows. However, such an exponential relationship fails to describe the hysteresis loop of the velocity, which was found by some authors. These authors showed that the velocity of the investigated earth flows proved to be higher during the rising limb of the groundwater than during the falling limb.

To explain the hysteresis loop in the velocity pattern, this paper considers the role of excess pore pressure in the rheological behaviour of earth flows by means of a mechanistic model. It describes changes in lateral internal stresses due to a change in the velocity of the earth flow, which generates excess pore pressure followed by pore pressure dissipation. Model results are compared with a hysteresis in the velocity pattern, which was measured on the Valette landslide complex (French Alps). Copyright © 2005 John Wiley & Sons, Ltd.

**Keywords:** earth flows; excess pore pressure; hysteresis; velocity

Received 14 July 2003;  
Revised 14 July 2004;  
Accepted 2 September 2004

## Introduction

There are many complex mass movements, which have a source area where blocks fail as rotational slides. These sliding blocks transform downslope into elongated flows with high water contents at or above the liquid limit, high velocities from 3 m per minute to 1.8 m per hour and flowing all over the vertical profile. These flows can be classified according to Hungr *et al.* (2001) as mud flows. At a later stage these flows transform into slower plug flow movements, which are classified by Hungr *et al.* (2001) as earth flows. These earth flows may move over a relatively thin viscous shear band with a high water content and a more or less rigid landslide body on top (Giusti *et al.*, 1996; Angeli *et al.*, 1998).

In the case of small groundwater fluctuations, the velocity of these slow-moving landslides can be described by Bingham's law with a linear relation between velocity as a function of excess shear stress and a constant dynamic viscosity (Van Asch and Van Genuchten, 1990; Angeli *et al.*, 1998). Many authors state that in most cases a non-linear version of Bingham's law best describes the moving pattern of these earth flows (Vulliet and Hutter, 1988). However, such an exponential relationship fails to describe the hysteresis loop in the velocity pattern, which was found by Bertini *et al.* (1986), Malet *et al.* (2002) and Malet (2003). These authors showed that the velocity of the investigated earth flow proved to be higher during the rising limb of the groundwater than during the falling limb.

Field evidence supports the hypothesis that earth flows cannot be considered as uniform rigid bodies and internal deformation accounts for the generation of excess pore pressures under initially undrained conditions (Giusti *et al.*, 1996). Zones of compression and extension may develop during movement, which results in positive or negative volumetric strain and hence the generation of negative or positive excess pore pressures (Picarelli *et al.*, 1995), followed by a dissipation of excess pore pressure.

Based on these findings, there is a strong case for the consideration of the role of excess pore pressure in the rheological behaviour of earth flows by means of a mechanistic model. An attempt will be described in this paper.

Model results will be compared with a hysteresis in the velocity pattern measured on the Valette earth flow in the Barcelonnette basin (French Alps).

### Hysteresis in the Velocity Patterns of the Valette Earth Flow

The mass movement complex of La Valette near Barcelonnette in the French Alps amounts to a volume of 3.6 million m<sup>3</sup> (Van Beek and Van Asch, 1996). It consists of a rotational block (50 m in depth) incorporating *in-situ* Flysch and Terres Noires rock material, which failed in March 1982 in the upper part (Figure 1). The middle part consists of meta-stable weathered Terres Noires and argillaceous morainic material. This part became active in 1986. Rapid slides in the middle part transformed into a mud flow and later into an earth flow according to the classification of Hungr *et al.* (2001). It built up the lower part of the landslide complex. The upper scarp of the landslide complex is situated at a height of 2000 m while the toe lies at 1250 m. The analyses are concentrated on the movement in the middle part where the material moved over a depth of 20 m with a slope of 18°. The type of movement can be characterized as a translational earth flow. Displacements at the surface were measured every one to two weeks along a survey line with 20 markers roughly perpendicular to the direction of movement (see Figure 1). The position of the markers was measured by a theodolite with an accuracy in the order of millimetres.

Hydraulic heads were measured with an open standpipe piezometer, about 20 m upslope of the survey line (Figure 1). The open standpipe piezometer (Ø 25 mm, 40 cm filter length) was installed according to standard procedures (Graig, 1992). The total head of the groundwater was calculated for a reference level at the depth of the slip surface, which is about 20 m below the topographical surface.

The data set analysed here covers the period from 9 September 1988 until 10 September 1991. The material in the middle part of the landslides consists of strongly remoulded Terres Noires mixed with morainic deposits. The matrix of this material is fine sandy silts with a considerable clay fraction in which large fragments (stones, gravel) are incorporated. Peak strength measured with triaxial tests in undisturbed morainic material amounts to  $\phi_p = 26.8^\circ$  ( $n = 10$ ,  $R^2 = 0.98$ ); the peak cohesion is relatively low: 2 kPa). After failure, strain softening was observed. With a strain of 16 per cent the incomplete residual strength for four samples ( $R^2 = 0.95$ ) has a residual friction value of  $\phi_r = 23.5^\circ$  (cohesion is assumed to be zero). Maquaire *et al.* (2003) measured strength values in reworked black marl formation on the Valette earth flow with  $\phi_p$  values between 21 and 24° and much higher cohesive values between 31 and 40 kPa, measured with direct shear tests.  $\phi_r$ -Ring shear values varied between 19 and 21° while the  $c_r$  values peculiarly remain rather high between 10 and 14 kPa.

In Figure 2 the measured velocity is plotted against the total head. The figure shows a nearly symmetric shape of the velocity graph while the rising and falling limbs of the total head level are asymmetric. The peak with the maximum rise in piezometric level shows clearly that velocities are higher for the same level in a rising limb than in a falling limb. This graph cannot be described with a non-linear rheological model. Therefore a rheological model is proposed here that explicitly generates excess pore pressure and that must describe the velocity pattern more truthfully.

### A Rheological Model with Excess Pore Pressure

In this model, velocity will be defined as a function of (a) excess shear stress, (b) an intrinsic constant viscosity, and (c) changing excess pore pressure conditions during movement.

Local changes in instability within segments of the earth flow will be resolved into changes in total inter-laminar lateral stress. Assuming initial undrained conditions, this lateral thrust is translated into changes in pore pressure followed by a dissipation of pore pressure. Resulting volumetric strains are ignored in the model. Only changes in stress during movement are considered. Velocity will be described by a visco-plastic model (Bingham's law) for the viscous shear band.

The computation starts with the determination of the overall safety factor ( $F$  for  $t = 1$ ) in the first time step according to Janbu's simplified method (Nash, 1987):

$$F^t = \frac{\sum \{c'L + [W^t - (U_{\text{normal}}^t + U_{\text{excess}}^t)] \tan \phi'\} / n_\alpha}{\sum W^t \tan \alpha} = \frac{\sum S}{\sum T} \quad (1a)$$

$$n_\alpha = \cos^2 \alpha \left( 1 + \tan \alpha \frac{\tan \phi'}{F^{t-1}} \right) \quad (1b)$$

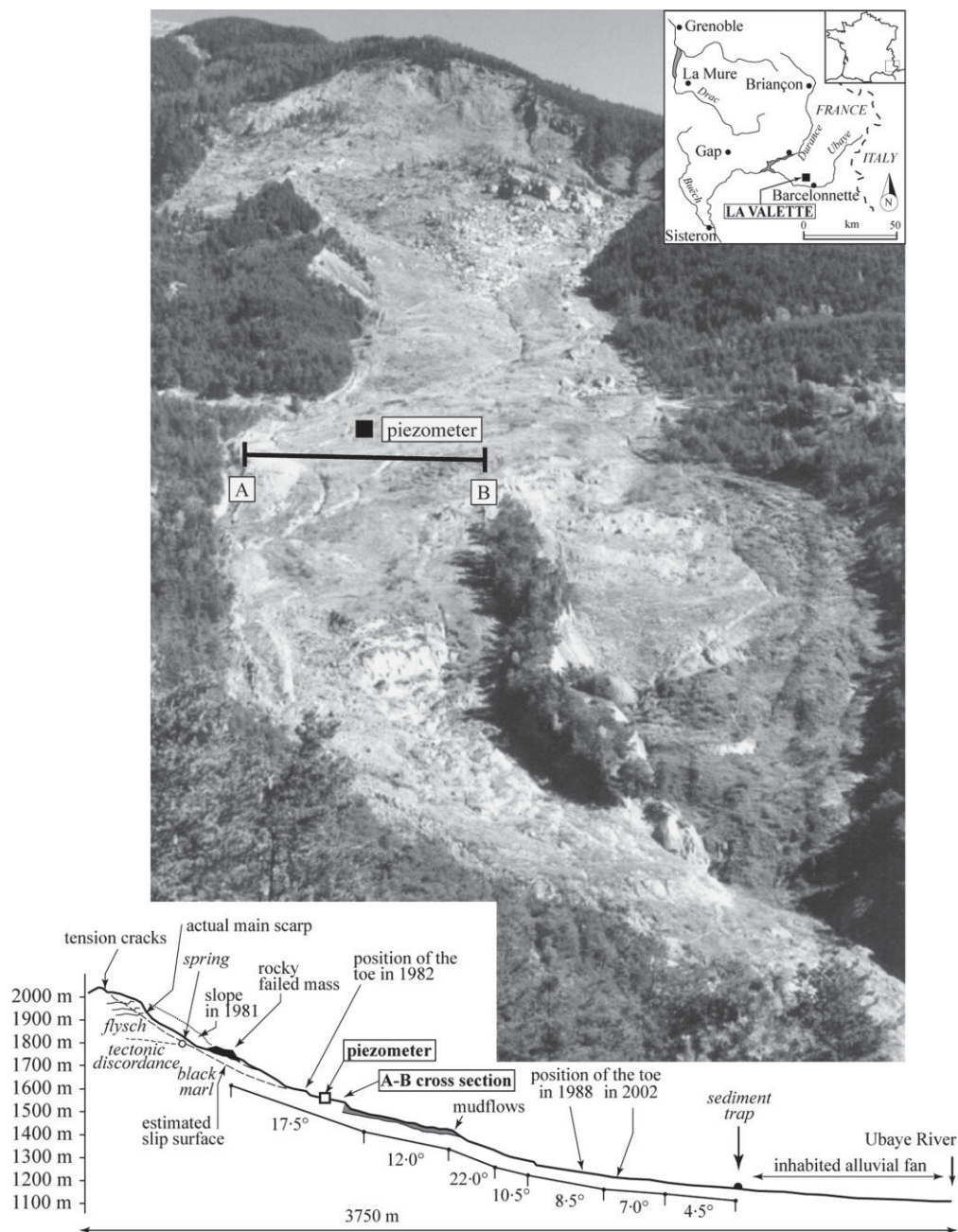


**Figure 1.** Photograph and a cross-section of the Valette landslide near Barcelonnette (French Alps). A–B marks the position where velocities were measured.

where (see also Figure 3)  $W$  = the weight of an individual slice  $i$  (for practical reasons the suffix  $i$  is omitted in the equations),  $U_{\text{normal}}$  = the pore water force on the slip surface of slice  $i$ , caused by height of groundwater,  $U_{\text{excess}}$  = excess pore pressure due to undrained lateral loading during movement (see below;  $U_{\text{excess}} = 0$  in the first time step),  $c'$  = is the cohesion (in kPa),  $\phi'$  = the friction angle of the material,  $\alpha$  = slope angle of slice  $i$ ,  $L$  = the length of the slip surface of slice  $i$ ,  $S$  = the resisting force of slice  $i$ ,  $T$  = the driving force of slice  $i$ .

Since the depth/length ratio of this long elongated earth flow is very small no correction factor is applied for the calculation of  $F$  (Nash, 1987).

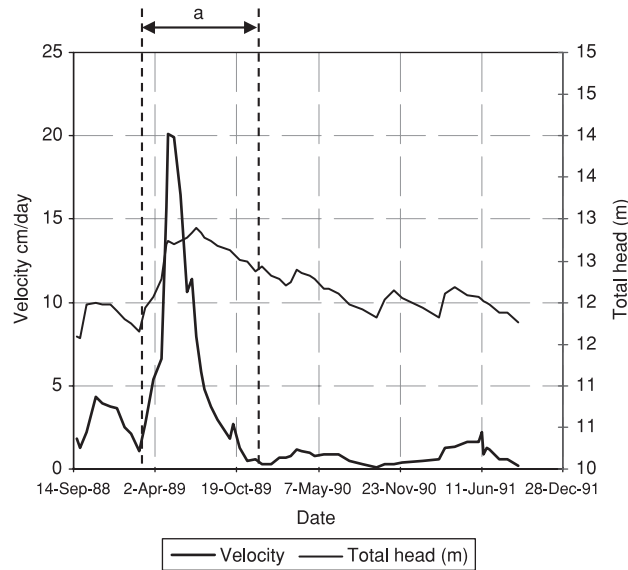


**Figure 2.** The relation between superficial velocity and total head of the groundwater in the Valette earth flow, for respectively rising and falling limbs from 9 September 1988 until 10 September 1991. The calibration period is labelled 'a'.

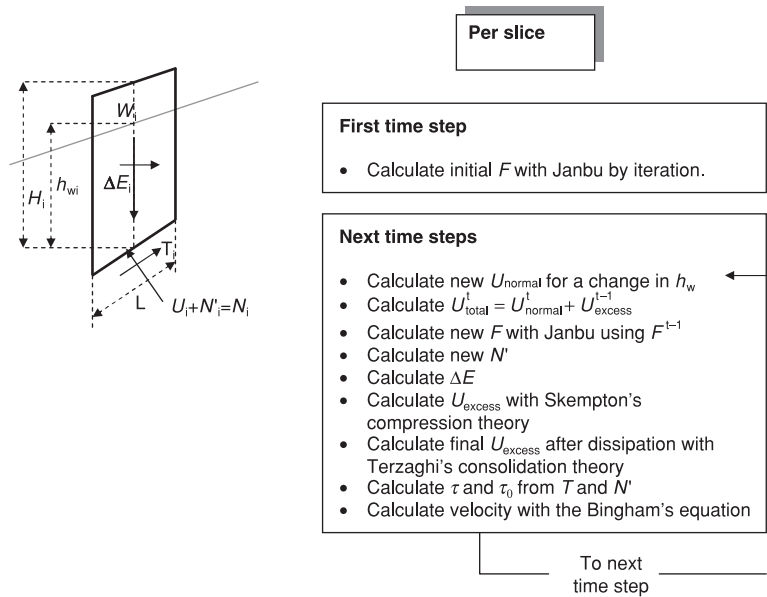


**Figure 3.** A modelling scheme for the calculation of excess pore pressure and velocity of an earth flow.

Equation 1 contains  $F$  on both sides, which is solved iteratively in the first time step. In the following time steps when the landslide is moving and groundwater level is changing, the new  $F^t$  on the left side of Equation 1a is calculated with  $F^{t-1}$  obtained from the former time step and this is substituted for each slice in Equation 1b to calculate the right side of Equation 1a.

The 'normal' pore pressure  $U$ , which is attributed to the height of the groundwater level flowing more or less parallel to the slip surface is given by:

$$U_{\text{normal}}^t = U_{\text{normal}}^{t-1} + \Delta h^t \cos^2 \alpha L \quad (2)$$

where  $\Delta h^t$  is the vertical rise of the groundwater above the slip surface at time step  $t$  (Figure 3).

The total pore pressure *at the beginning of the time step* is the sum of the normal pore pressure given by the height of the groundwater in the current time step and the excess pore pressure calculated (see below) in the foregoing time step.

$$U_{\text{total}}^t = U_{\text{normal}}^t + U_{\text{excess}}^{t-1} \quad (3)$$

It is assumed that the excess pore water force ( $U_{\text{excess}}^t$ ) is generated during movement due to a change in the net lateral force  $\Delta E$  (see Figure 3) between two time steps by the principle of undrained loading.

In order to calculate  $\Delta E$  for each slice for a given time step, forces are resolved vertically to calculate the total normal force  $N$  for each slice (see Figure 3):

$$N^t = \left[ W^t - \frac{1}{F^{t-1}} (c'L \sin \alpha - U_{\text{total}}^t \tan \phi' \sin \alpha) \right] / m_\alpha \quad (4)$$

where

$$m_\alpha = \cos \alpha \left( 1 + \tan \alpha \frac{\tan \phi'}{F^{t-1}} \right) \quad (5)$$

Resolving the forces parallel to the slip surface for each slice delivers  $\Delta E$ :

$$\Delta E^t = W^t \tan \alpha - \frac{1}{F^{t-1}} [c'L + (N^t - U_{\text{total}}^t) \tan \phi'] \sec \alpha \quad (6)$$

It is assumed that a change in the net inter-slice forces ( $\Delta E^t - \Delta E^{t-1}$ ) (see Figure 3) between two time steps creates the excess pore pressure and therefore:

$$U_{\text{excess}}^t = U_{\text{excess}}^{t-1} + (\Delta E^t - \Delta E^{t-1}) - A(\Delta E^t - \Delta E^{t-1}) \quad (7)$$

where  $A$  is related to Skempton's pore pressure coefficient (Whitlow, 1995).

During the time step there is also dissipation of pore pressure. An average fractional loss ( $Fr$ ) of  $U_{\text{excess}}^t$  during a time step can be obtained using Therzaghi's theory of consolidation for a half closed layer (assuming an impermeable slip surface, vertical drainage upwards and one-dimensional consolidation (Whitlow, 1995):

$$Fr = 1 - \frac{16}{\pi^3} \left[ (\pi - 2)e^{-(\pi^2/4)T_v} + \frac{1}{27}(3\pi - 2)e^{-(9\pi^2/4)T_v} + \frac{1}{125}(5\pi - 2)e^{-(25\pi^2/4)T_v} \dots \right] \quad (8)$$

where  $T_v$  is the dimensionless time factor of the consolidation and pore water dissipation process.  $Fr$  has a value between 0 and 1 (= complete dissipation of excess pore pressure).

$T_v$  in Equation 8 is defined as follows:

$$T_v = \frac{C_v t}{d^2} \quad (9)$$

where  $t$  is time (day);  $d$  is the length (m) of the drainage path which for a half-closed layer equals the thickness of the water layer or in our case the saturated height  $h_w$  of the slice.  $C_v$  is the coefficient of consolidation ( $\text{m}^2 \text{day}^{-1}$ ):

$$C_v = \frac{k}{m_v \gamma_w} \quad (10)$$

where  $m_v$  is the coefficient of volume compressibility ( $\text{m}^2 \text{kN}^{-1}$ ),  $k$  the saturated hydraulic conductivity ( $\text{m day}^{-1}$ ) and  $\gamma_w$  the unit weight of water ( $\text{kN m}^{-3}$ ).

The new  $U_{\text{excess}}^t$  at the end of the time step after consolidation becomes:

$$U_{\text{excess}}^t = U_{\text{excess}}^{t-1} - Fr U_{\text{excess}}^{t-1} \quad (11)$$

This value is used in the next time step to calculate the new  $U_{\text{total}}$  (see Equation 3).

The shear stress ( $\bar{\tau}$ ) and shear strength  $\bar{\tau}_0$  along the length of the slip surface of one slice is used to calculate the velocity of the earth flow:

$$\tau_0 = \frac{S}{L} \quad \tau = \frac{T}{L} \quad (12)$$

where  $S$  and  $T$  are given by Equation 1a.

The velocity is calculated according to Bingham's law:

$$v = \frac{h_m}{\eta}(\tau - \tau_0) \quad (13)$$

where  $v$  is the velocity ( $\text{m s}^{-1}$ ),  $h_m$  is the thickness of the shear band (m),  $\eta$  is the dynamic viscosity ( $\text{kPa s}$ ). Here the velocity ( $v$ ) is a linear function of the excess shear stress ( $\tau - \tau_0$ ) and not an exponential function. Our hypothesis is that the exponential behaviour is caused by the development of excess pore pressure, which means that there is a non-linear behaviour of  $S$  (or  $\tau_0$ ), as a function of  $U_{\text{excess}}$  during movement (see Equations 1a, 12 and 13).

### Calibration of the Model on the Valette Landslide

The highest peak in the velocity of the Valette Earth flow was selected to calibrate the model. A rising limb with sufficient data points was available during the period 22 February 1989 until 13 July 1989 and a falling limb was obtained from the period 14 July 1989 until 12 January 1990 (Figure 2). Table I shows an overview of the parameters that were used in the model.

The table shows that calibration was carried out on two parameters: the ratio between shear band thickness and viscosity  $h_m/\eta$  (Equation 13) and Skempton's pore pressure coefficient  $A$  (Equation 7). Figure 4 shows that the first velocity peak could be modelled rather well. The model reacts sharply with a second peak on a further but slighter

**Table I.** Measured and calibrated parametric values for the excess pore pressure model

Parameter	Value	Remark
Residual cohesion $C_r$ shear band	$\sim 0$ kPa	Ring shear tests
Friction angle $\phi_r$ (-) shear band	$23.5^\circ$	Ring shear tests
Thickness shear band / dynamic viscosity, $h_m/\eta$ (Equation 13)	$8\text{E-}7$ $\text{m kN}^{-1} \text{s}^{-1}$	Calibration
$C_v$ = coefficient of consolidation (Equation 10)	$17.5$ $\text{m}^2 \text{day}^{-1}$	Oedometer tests
Skempton's pore pressure coefficient $A$ (Equation 7)	0.6	Calibration
Bulk density	$18.2$ $\text{kN m}^{-3}$	Laboratory measurements

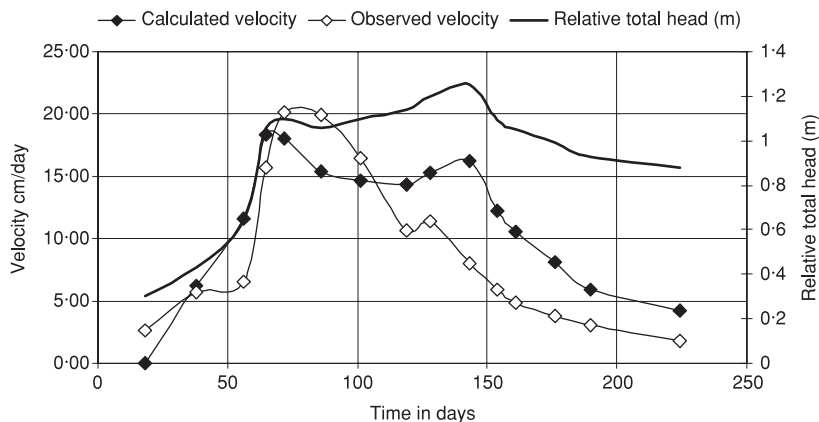


**Figure 4.** Measured and calculated velocities of the Valette earth flow.

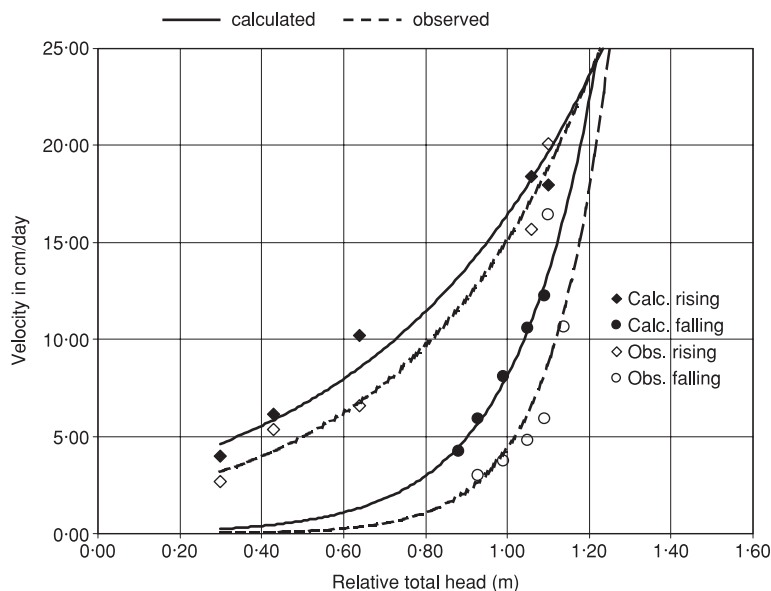


**Figure 5.** The measured and calculated hysteresis in the velocity pattern of the Valette earth flow.

increase and decrease of the piezometric level. The observed velocity of the landslide shows only a minor peak. The response is less severe as predicted by the model. However, both the observed and calculated velocities show an asymmetric relationship with fluctuation of the piezometric level. This is better demonstrated in Figure 5, which clearly shows a hysteresis of the trendlines of measured and calculated velocities for a rising and falling limb of the piezometric level.

### Sensitivity Analyses

A sensitivity analysis was carried out for Skempton's pore pressure coefficient  $A$  (Equation 7) and for  $C_v$ , (see Equations 8–10). An index is defined for the effect of these parameters on the hysteresis pattern. This is the maximum difference in velocity which is found between a rising and falling limb for a given groundwater level. The two parametric values were fixed at a mean given in Table I. Each parameter was consecutively increased and decreased stepwise towards a maximum of 50 per cent. Figure 6 shows the results.

Skempton's pore pressure coefficient  $A$  proved to be the most sensitive parameter for the given range in parametric values.

### Discussion and Conclusions

A velocity as a non-linear function of excess shear stress and viscosity commonly describes the velocity pattern of complex earth flows experiencing visco-plastic deformation. The driving excess shear stress is related directly to a decrease in effective stress, i.e. an increase in pore pressure. However, it has been demonstrated that for actual earth flows existing models describing this relationship do not explain a hysteresis in the velocity between a rising and falling groundwater limb. This hysteresis should be ascribed to the generation of excess pore pressure or suction due to respectively compression and decompression. As an amendment to existing models a simple model has been developed that includes the generation of excess pore pressure and its dissipation during movement. It describes changes in lateral stresses due to changes in velocity. The model presented shows a hysteresis in the velocity pattern, which was found in the Valette earth flows as well as in other slides. Therefore the inclusion of excess pore pressure seems to be realistic.

The generation of excess pore pressure is the most common feature for explaining the fluidization and large runout distances of landslides. The most widely known and abundantly studied feature is the effect of loose highly porous

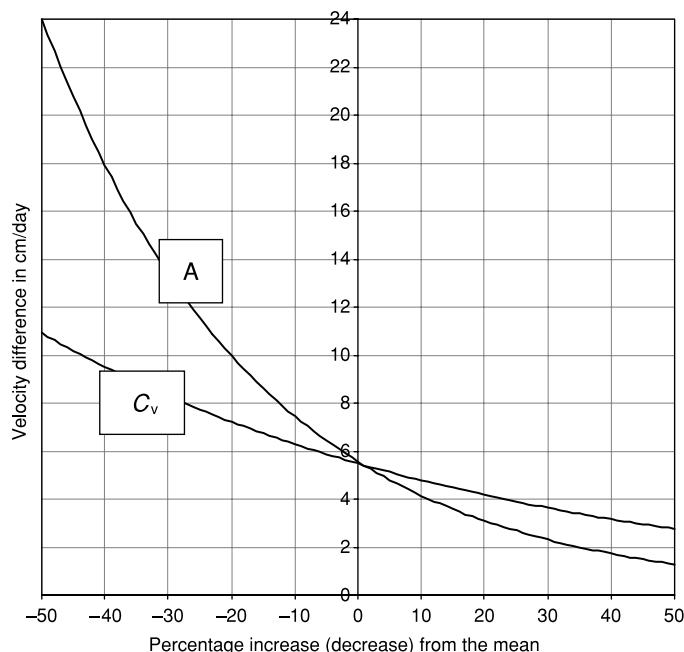


**Figure 6.** The effect of two parametric values on the hysteresis index (see text): A is Skempton's pore pressure coefficient;  $C_v$  is the coefficient of consolidation ( $\text{m}^2 \text{day}^{-1}$ ).

soil (like volcanic ash), which compacts during initial failure, generating excess pore pressure (Yoshimimi *et al.*, 1989; Anderson and Riemer, 1995; Fuchu Dai *et al.*, 1999; Okura *et al.*, 2002). Also particle breakage may occur along the slip surface of rapidly moving slides, causing contraction of the soil and generating excess pore pressure and liquefaction in the slip surface (Sassa, 1998; Wang *et al.*, 2002).

In slow-moving complex earth flows the inclusion of excess pore pressure must also be considered. In this case zones of compression and extension due to changes in velocity and loading of new failing blocks in the steeper source area generate excess pressures. Under critical conditions, these earth flows may generate rapid surges or transform into mud flows through fluidization. Such changes in the rheological behaviour are extremely dangerous for human life or activities in the possible path of the earth flow. Presently, models to predict such changes for existing landslides are based on observations of displacement and groundwater levels that seldom include observations within this critical range. Such predictions will be unreliable if they are applied outside the range of measured velocities. The inclusion of excess pore pressure in the proposed model will provide the possibility of evaluating such conditions deterministically and with more reliability.

## References

- Anderson SA, Riemer MF. 1995. Collapse of saturated soil due to reduction in confinement. *Journal of Geotechnical Engineering, ASCE* **121**(2): 216–220.
- Angeli MG, Buma J, Gasparetto P, Pasuto A. 1998. A combined hill slope hydrology/stability model for low-gradient slopes in the Italian Dolomites. *Engineering Geology* **49**: 1–13.
- Bertini T, Cugusi F, Délia B, Rossi-Doria M. 1986. Lenti movimenti di versante nell'Abruzzo Adriatico: caratteri e criteri di stabilizzazione. *16th Convegno Nazionale di geotecnica, Bologna* **1**: 91–100.
- Fuchu Dai Lee CF, Sijing Wang, Yuong Feng. 1999. Stress-strain behaviour of loosely compacted volcanic-derived soil and its significance to rainfall-induced fill slope failures. *Engineering Geology* **53**: 359–370.
- Giusti G, Lacarino G, Pellegrino A, Russo C, Urcioli G, Picarelli L. 1996. Kinematic features of Earth flows in Southern Apennines, Italy. In *Proceedings of the VIIth International Symposium on Landslides, Trondheim* vol. 1, Senneset (ed.). Balkema: Rotterdam; 457–462.
- Graig RF. 1992. *Soil Mechanics*. Chapman & Hall: London.
- Hungr O, Evans SG, Bovis MJ, Hutchinson JN. 2001. A review of the classification of landslides of the flow type. *Environmental and Engineering Geoscience* **VII**(3): 221–238.



- Malet J-P. 2003. *Les 'glissements de type écoulement' dans les marnes noires des Alpes du Sud. Morphologie, fonctionnement et modélisation hydro-mécanique*. Doctoral thesis, University Louis Pasteur, Strasbourg.
- Malet J-P, Maquaire O, Calais E. 2002. The use of Global Positioning System techniques for continuous monitoring of landslides: application to the Super-Sauze Earth flow (Alpes-de Haute-Provence, France). *Geomorphology* **43**(1–2): 33–54.
- Maquaire O, Malet J-P, Remaître A, Locat J, Klotz S, Guillon J. 2003. Instability conditions of marly hillslopes: towards landsliding or gullyng? The case of the Barcelonnette basin, South East France. *Engineering Geology* **70**: 109–130.
- Nash DFT. 1987. A comparative review of limit equilibrium methods of stability analysis. In *Slope Stability, Geotechnical Engineering and Geomorphology*, Anderson MG, Richards KS (eds). John Wiley & Sons: Chichester; 11–77.
- Okura Y, Kithahara H, Ochiai H, Sammori T, Kawanami A. 2002. Landslide fluidisation process by flume experiments. *Engineering Geology* **66**: 65–78.
- Picarelli L, Russo C, Urcioli G. 1995. Modelling earthflow movement based on experiences. *11th European Conference on Soil Mechanics and Foundation Engineering, Copenhagen* **6**: 157–162.
- Sassa K. 1998. Mechanisms of landslide triggered debris flow. In *Environmental Forest Science*, Sassa K (ed.). Kluwer Academic Publishing: Dordrecht; 471–490.
- Van Asch TWJ, Van Genuchten PMB. 1990. A comparison between theoretical and measured creep profiles of landslides. *Geomorphology* **3**: 45–55.
- Van Beek LPH, Van Asch TWJ. 1996. The mobility characteristics of the Valette landslide. In *Proceedings of the VIIth International Symposium on Landslides, Trondheim* vol. 2, Senneset (ed.). Balkema: Rotterdam; 1417–1421.
- Vulliet L, Hutter K. 1988. Viscous-type sliding laws for landslides. *Canadian Geotechnical Journal* **25**: 467–477.
- Wang FW, Sassa K, Gonghui Wang. 2002. Mechanism of a long run out landslide triggered by the August heavy rainfall in Fukushima Prefecture Japan. *Engineering Geology* **63**: 169–185.
- Whitlow R. 1995. *Basic Soil Mechanics*. Longman: Essex.
- Yoshimimi Y, Tanaka K, Tokimatsu K. 1989. Liquefaction resistance of partially saturated sand. *Journal of Soil and Foundation Engineering* **29**(3): 157–162.